Green's function method for calculation of adsorption of organic molecules on noble metal nanoparticles

O. V. Farberovich,[1,2] B. D. Fainberg,[1,3] V. G. Maslov,[4] and V. Fleurov[2,5]

[1]*Faculty of Sciences, Holon Institute of Technology, 52 Golomb Street, Holon IL-58102, Israel*

[2]*Raymond and Beverly Sackler Faculty of Exact Sciences, School of Physics and Astronomy, Tel-Aviv University, Tel-Aviv IL-69978, Israel*

[3]*Raymond and Beverly Sackler Faculty of Exact Sciences, School of Chemistry, Tel-Aviv University, Tel-Aviv IL-69978, Israel*

[4]*Saint Petersburg State University of Information and Technologies, Mechanics and Optics, Saint Petersburg 197101, Russia*

[5]*Max-Planck-Institut für Physik Komplexer Systeme, Nöthnitzer Strasse 38, 01187 Dresden, Germany*

(Received 13 September 2010; revised manuscript received 18 November 2010; published 23 February 2011)

A numerical method for the calculation of electronic structure of a nanosystem composed of a pseudoisocyanine (PIC) molecule assembled on a silver nanoparticle is developed. The electronic structure of the silver nanoparticle containing 125 atoms is calculated within the local density version of the density functional method. A model of an Ag atom embedded in the center of a spherical jellium cluster is used. The host electron Green's function is calculated by means of the spherically symmetric expansion. The principal theoretical tool is the scattering theory using the Green's function method. The molecule-silver nanosystem interaction is studied using the approach similar to that of the Anderson model for transition metal impurities in solids. Localized levels are shown to split off from the top of the band of the Ag nanoparticle. The electronic structure calculations yield information on the character of chemical bonding in the PIC molecule-silver particle nanosystem.

DOI: 10.1103/PhysRevB.83.085420 PACS number(s): 73.22.−f, 36.40.−c, 31.15.−p

I. INTRODUCTION

Organic-inorganic nanohybrid materials that utilize noble metals (silver or gold), functionalized with organic or biological constituents can produce unique physical and chemical properties that otherwise are not possible in single component materials.[1] These materials have given rise to a growing interest in theoretical methods that can calculate the electronic structure and transport properties of nanoscale devices.[2–4] A major problem with these nanostructures is to optically control molecular self-organization on metallic surface. J-aggregates of cyanine dyes make a fascinating topic of research due to their outstanding optical properties.[5] Spectroscopic peculiarities are the result of exceptionally strong electronic interactions between the transition dipole moments of the dyes that give rise to extended exciton states after photo excitation.[4] The excitonic optical spectrum depends on the details of the structural and electronic arrangement of the dye molecule.[6]

The adsorption of dyes to nanoparticles of noble metals presents a special interest.[7] The study of the interaction of an adsorbed dye, in both its ground and excited states, with the energy states of the conduction band of metal is also of interest and may rely on theoretical calculations of the energy electronic structure of the nanosystem made of *pseudoisocyanine* (PIC) *assembled on a silver nanoparticle*. Moreover, the nature of coupling between excitonic molecular J-aggregates and a metallic nanoparticle is still not completely understood since, to the best of our knowledge, no attempts have been made to calculate the electronic structure of Ag + PIC nanosystems from the "first principles." In addition, a major problem of molecular engineering is to control molecular self-organization.[8] This process is governed by the formation of chemical bonds (e.g., covalent or hydrogen bonds). The assembly process on nanoparticles is also affected by the molecule-substrate interactions. Therefore, understanding bonding between the molecules and nanoparticle is crucial to be able to choose appropriately the molecular and substrate materials for a nanosystem design. On the theoretical side, the new computational techniques allow one to predict the preferential geometry of the nanostructure arrangements as well as the strength and chemical bonds involved directly from the fundamental quantum mechanical laws.

We demonstrate how *ab initio* calculations allow one to explain the shape of the observed superstructures, to elucidate the role of electronic structure and the molecule-silver particle bonding and to reveal details of the nanosystems not yet experimentally accessible.

Quantum electronic-structure calculations allow us to understand the macroscopic properties of complex polyatomic systems (specifically, the organic PIC molecule assembled on a silver nanoparticle) in terms of the microscopic states available to the electrons described by their wave functions and the nanosystem electron density $\rho^{\text{nano}}(\mathbf{r})$. For these larger systems it is frequently of a greater interest to know the change in the electronic-structure associated with the changes in the Kohn-Sham[9] effective potential $V_{\text{eff}}(\mathbf{r})$ and the electron density. Our work develops a theoretical technique that makes the direct calculation of such changes possible. This technique is based on the self-consistent Green's function method[10] and standard density-functional theory (DFT) in combination with the *local-density approximation* (LDA),[11] which maps the many-electron interaction problem onto a self-consistent treatment of noninteracting quasiparticles moving in an effective potential

$$V_{\text{eff}}(\mathbf{r}) = V_{\text{ext}}(\mathbf{r}) + 2\int \frac{\rho^{\text{nano}}(\mathbf{r}')}{|\mathbf{r}-\mathbf{r}'|}d\mathbf{r}' + V_{\text{xc}}(\mathbf{r}), \qquad (1)$$

where $V_{\text{ext}}(\mathbf{r})$ is the external potential and $V_{\text{xc}}(\mathbf{r})$ is the local exchange-correlation potential.s

II. FORMULATION OF THE PROBLEM

We present in this paper results of numerical calculations of the electronic structure of a nanosystem: PIC molecule + small Ag particle whose electronic structure is described by

the Hamiltonian

$$H = H_{\text{jellium}} + H_{4d} + H_{\text{PIC}} + H^{p}_{\text{PIC}-\text{Ag}} + H^{r}_{\text{PIC}-\text{Ag}}. \quad (2)$$

The first term stands for the spherical jellium cluster Hamiltonian made of 5*s*-valence electrons of an Ag atom. The next term in the Hamiltonian (2) describes the subsystem of Ag 4*d*-electrons embedded in the spherical jellium cluster. H_{PIC} stands for the PIC molecule Hamiltonian. The last two terms of the Hamiltonian (2) describe the *resonant* (r) (due to the presence of the 4*d* state of Ag atoms) and *potential* (p) (due to the Ag 5*s* states) scattering. This distinction between the two types of scatterring by atomic potential is discussed in detail in Ref. 12 (see also Ref. 10).

The method is based on the separation of the Hamiltonian (2) into the two parts

$$H = H^{0}_{\text{LDA}} + \Delta H. \quad (3)$$

Here $H^{0}_{\text{LDA}} = H_{\text{jellium}} + H_{4d}$ is the Hamiltonian of the *reference* system, which includes an effective single-particle LDA potential $V^{0}_{\text{LDA}}(\mathbf{r})$. $\Delta H = H_{\text{PIC}} + H^{p}_{\text{PIC}-\text{Ag}} + H^{r}_{\text{PIC}-\text{Ag}}$ is the Hamiltonian of the "difference" system described by the potential $\Delta V(\mathbf{r})$, which is the difference between the self-consistent Kohn-Sham (1) effective potential $V_{\text{eff}}(\mathbf{r})$ and $V^{0}_{\text{LDA}}(\mathbf{r})$.

Four different computation schemes are used, each of which provides mutually complementary information about the electronic spectra of the complex nanosystem. The first one is the spherical jellium cluster model with the central 4*d* Ag atom embedded in the center of a silver nanoparticle.[13] The second method is based on the Green's function approach. Then the physical effect shows up exclusively in variations of the Kohn-Sham effective potential $V_{\text{eff}}(\mathbf{r})$ (Ref. 9) and of the nanosystem electron density $\rho^{\text{nano}}(\mathbf{r})$. In this approach, we follow a two-step concept and split the entire problem into two parts where each of them is far less complicated than the original one.[14,15] The whole nanosystem is decomposed into the reference system characterized by the ground-state electron density $\rho^{0}_{\text{LDA}}(\mathbf{r})$ and the difference system with the electron density

$$\Delta\rho(\mathbf{r}) = \rho^{\text{nano}}(\mathbf{r}) - \rho^{0}_{\text{LDA}}(\mathbf{r}), \quad (4)$$

which is the difference between the self-consistent electron density $\rho^{\text{nano}}(\mathbf{r})$ of the nanosystem and the ground-state electron density $\rho^{0}_{\text{LDA}}(\mathbf{r})$ corresponding to the Hamiltonian

$$H^{0}_{\text{LDA}} = -\nabla^2 + V^{0}_{\text{LDA}}(\mathbf{r}) \quad (5)$$

(atomic Rydberg units are used). Here $H^{0}_{\text{LDA}} = H_{\text{jellium}} + H_{4d}$. The complete set of electronic states of the reference system is represented by the reference Green's operator

$$G^{0}(z) = \left(z - H^{0}_{\text{LDA}}\right)^{-1}, \quad (6)$$

depending on the complex variable $z = \varepsilon + i\eta(\eta \geqslant 0)$. The calculation of $G^{0}(z)$ along a properly chosen contour in the complex energy plane defines step one of our approach. As the second step, the Green's operator $G(z)$ of the nanocluster-assembled system (and the charge density related to it) is determined by solving the Dyson equation

$$G(z) = G^{0}(z) + G^{0}(z)\Delta V G(z), \quad (7)$$

in a self-consistent way. A detailed description of our approach to solving Eq. (7) is presented in the Appendix.

The third semi-empirical method Zerner's intermediate neglect of differential overlap (ZINDO/S)[16] was used for the calculation of the electronic structure of a neutral PIC molecule. The fourth DFT/B3LYP/6-31G[17] method was applied to the equilibrium geometry calculation of PIC molecule by the standard DFT method.

We would also like to indicate here the limitations of our approach to the treatment of the Ag + PIC nanosystem based on the spherical jellium model for the Ag nanoparticle. The previous structural research[18] using the method of the molecular dynamics shows that very diverse nonspherical geometries of the nanoparticle are possible. The relaxation of the PIC molecule and nanoparticle reconstruction in response to the PIC molecule are also not taken into account. Including all the processes into the calculation scheme can strongly complicate the procedure and we leave it for our future research.

III. CALCULATION OF THE ELECTRONIC STRUCTURE OF AG NANOPARTICLE

First, we consider the electronic structure of the silver nanoparticle. Cluster calculations are traditionally employed in studies of surface and bulk materials. They help us to understand how the physical properties evolve from a free atom to a finite-size system. In recent years, microclusters on the basis of Ag atoms attracted a lot of interest due to the growing technological significance of nanosystems including Ag and Au nanoparticles.[19,20] A variety of theoretical models have been proposed for the calculations of cluster electronic structure. However, the most precise models allow one to obtain their electronic structure with a small number of atoms only. For large atomic aggregations, these methods cannot be applied successfully, and simpler models are employed in this case. Thus, for the study of electronic properties of sp-bonded metal clusters, a jellium model is used.[21] But the models based on the jellium approximation are not directly suitable for the investigations of metal clusters containing atoms with localized *d* shells. As a consequence, a model of an *Ag atom embedded in the center of a spherical jellium cluster* is applied for a description of a small Ag metallic nanoparticle containing localized 4*d* electrons. The DFT approach in the LDA was used in the computation.[13,22] Each atom of the nanoparticle is mimicked by a single atom embedded in the center of a jellium sphere with the r_M radius, determined according to the position of the real atom with respect to the cluster surface. r_M is then the shortcut between the atom and the cluster surface.

The electronic structure of an Ag atom embedded in the jellium sphere is obtained within the DFT framework from a self-consistent solution of the Kohn-Sham equations (in atomic Rydberg units)[9,22]

$$\left[-\nabla^2 + V^{0}_{\text{LDA}}(\mathbf{r})\right]\psi_{nl}(\mathbf{r}) = \varepsilon_{nl}\psi_{nl}(\mathbf{r}), \quad (8)$$

where

$$V^0_{\rm LDA}(r) = -\frac{2Z^0}{r} + 2\int \frac{\rho^-(\mathbf{r}') - \rho^+(\mathbf{r}')}{|\mathbf{r}-\mathbf{r}'|}d\mathbf{r}' + V_{\rm xc}(r), \quad (9)$$

with the Vosko *et al.* form[23] of the local exchange-correlation potential $V_{\rm xc}(r)$. Here ε_{nl} and ψ_{nl} are single electron energies and wave functions, respectively; Z^0 is the nuclear charge of the Ag atom. The electron density of the jellium cluster with an Ag atom is

$$\rho^-(\mathbf{r}) = \sum_{nl} f_{nl}|\psi_{nl}(\mathbf{r})|^2, \quad (10)$$

where the coefficients f_{nl} are the occupation numbers of the states with quantum numbers n,l, and the summation is over all states of the *atom-in-jellium* nanoparticle. The radial distribution of the positive jellium background is given by

$$\rho^+(r) = \left[3N_{\rm val}(N_{at}-1)/4\pi r_M^3\right]\Theta(r_M - r), \quad (11)$$

where $\Theta(x)$ is the unit step function, $N_{\rm at}$ is the number of atoms in the cluster (including the specific Ag atom), $N_{\rm val}$ is the number of valence electrons in the Ag atom. The cluster radius r_M is found from the expression

$$r_M = N_{\rm at}^{1/3} r_c, \quad (12)$$

where r_c is the Wigner-Seitz radius. We have used here $r_c = 3.02356$ a.u., $N_{\rm at} = 125$, and $N_{\rm val} = 1$. The numerical integration of the Kohn-Sham equation for the Ag atom in a jellium sphere is carried out by means of the Milne method.[24] The free Ag atom eigenenergies ε_{nl} and wave functions ψ_{nl} are calculated by means of the semirelativistic RATOM program.[25] The self-consistency procedure for the potential $V^0_{\rm LDA}(r)$ is carried out in a mixed fashion. The first two iterations use the arithmetic average scheme, which later on is effectively substituted by the Aitken scheme.[26]

The electronic ground-state configurations of the jellium sphere containing the central Ag atom were determined in the following way. The rules for the energy level occupation separately in jellium and in a free atom are well known. Clearly, insertion of an atom into the jellium sphere center does not change the atom and jellium field symmetry, and consequently, the symmetry of their electronic states is not changed either. One can suppose therefore that the number of electron states with the same symmetry in the jellium sphere with the central atom is equal to the sum of such symmetry states of the jellium and the atom. The sequence of energy levels of *atom-in-jellium* is obtained by solving the self-consistent equations (8)–(10) for the different angular l and principal n quantum numbers. The energy levels are occupied in accordance with the Pauli principle. The highest levels can be partially occupied.

We have computed the total energy of the jellium spheres with the Ag atom in the center for various occupation numbers of the upper levels. For the calculation of the total energy we employed the equation

$$E_{\rm tot} = \sum_j^{\rm occ}\varepsilon_j + \int \rho^-_{\rm out}(\mathbf{r}) \times \left[\varepsilon^{\rm out}_{\rm xc}(\mathbf{r}) - V^{\rm in}_{\rm xc}(\mathbf{r}) + \int \frac{\rho^-_{\rm out}(\mathbf{r}') - 2\rho^-_{\rm in}(\mathbf{r}')}{|\mathbf{r}-\mathbf{r}'|}d\mathbf{r}'\right]d\mathbf{r}. \quad (13)$$

Here the indices *in* and *out* indicate the input and output data of the latest self-consistency iteration, respectively; $\varepsilon^{\rm out}_{\rm xc}(\mathbf{r})$ is the exchange-correlation energy density of a homogeneous electron gas with the density $\rho^-_{\rm out}(\mathbf{r})$ parameterized according to Vosko *et al.*[23]

The calculations have shown that the spherical jellium nanoparticle with the central $4d$ Ag atom has the following energy spectrum. The eight lowest energy levels are identical to those of the $4d$ atom core; the rest of them are similar to the states in a spherical potential well. In this paper the quantity $n = n_n + 1$ has been considered as the principal quantum number; n_n is the number of nodes of the wave function of the corresponding energy level. Thus, the electronic configuration of the central Ag atom in the jellium sphere is $1s^2 2s^2 1p^6 3s^2 2p^6 1d^{10} 4s^2 3p^6$. The electronic states of the 125 atoms are arranged in the following order: $2d^{10} 1f^{14} 1g^{18} 1h^{22} 2f^{14} 1i^{26} 1j^{30}$. The self-consistent potential $V^0_{\rm LDA}(r)$ [Eq.(9)] with the electronic levels for an Ag atom embedded in a jellium sphere is presented in Fig. 1.

An important characteristic of the Ag nanoparticles is their ionization potential (IP). It has been shown in Ref. 27 that a strong correlation exists between the chemisorption reactivity of a small transition metal cluster and its ionization threshold. Here we report the IP's for the Ag nanoparticles contain up to 160 atoms. In these calculations we simulate atoms of an Ag nanoparticle by Ag atoms embedded in the center of jellium spheres of various sizes. The jellium sphere radius r_M is defined by the shortcut between the atom and the cluster surface.

The IP of an *atom-in-jellium* was obtained using the ground-state theory (LDA method) by self-consistent calculation according to Eq. (13) and subtraction of the total energies of neutral and ionic ground states. It was found that the ionization thresholds of atoms of the Ag nanoparticles differ and depend on the position of the atoms with respect to the cluster surface. The lowest atomic ionization threshold has been chosen as the IP of the Ag nanoparticle. For the neutral Ag atom we

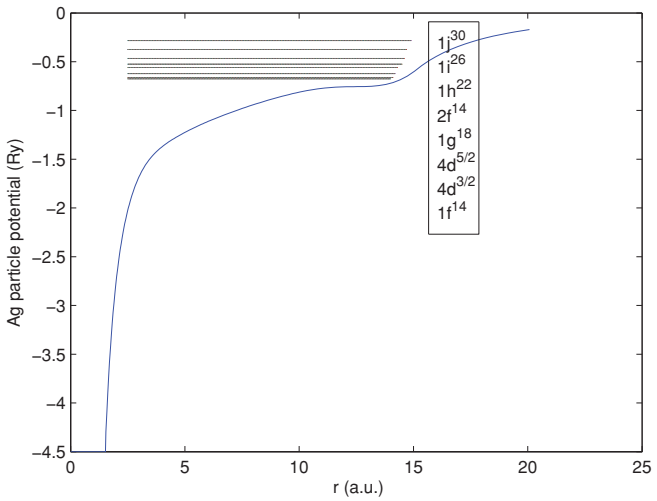

FIG. 1. (Color online) A self-consistent Ag-nanoparticle potential of the jellium sphere containing the central Ag atom (the radial distribution, in atomic units). The states of subshell $2d^{10}$ are split into $4d^{5/2}$ and $4d^{3/2}$ levels due to the spin-orbit interaction.

obtained $IP_{atom}^{theor} = 7.96$ eV and $IP_{atom}^{exp} = 7.576$ eV. Instead of calculating the IP's from the data as the total energy differences between the neutral cluster and ions, we use an alternative method based on the Slater transition state approach[28] and Janak theorem[29] for the DFT, which allows us to calculate the excitation energy of adding (removing) an electron to (from) the system from (to) the infinity. This scheme can be derived in the following way. The total energy E_{tot} difference between the final and initial states for the process of electron addition to the one-electron state j can be calculated as an integral of total energy derivative with respect to the occupancy q_j. This derivative, $\varepsilon_j = \partial E/\partial q_j$, corresponds to the Kohn-Sham eigenvalue

$$E(q_j = 1) - E(q_j = 0) = \int_0^1 dq_j \varepsilon_j(q_j) \simeq \varepsilon_j(0.5). \quad (14)$$

Equation (14) becomes exact if the LDA eigenvalue $\varepsilon_j(q_j)$ is a linear function of the occupancy, which is usually true to within a good accuracy.

The vertical (or adiabatic) ionization potentials[30] of the clusters are evaluated from the *highest occupied molecular orbital* (HOMO) energy of the neutral clusters. The calculated IP of an Ag_{125} nanoparticle is $IP^{theor} = 4.73$ eV. When the number of atoms in the nanoparticle increases the IP converges to the work function Φ of the corresponding metallic half-space. The work function of 4.46 eV was determined experimentally for Ag(111) (Ref. 31). Our calculation yields the value of 4.73 eV for IP_{125}^{theor}. The LDA HOMO-lowest unoccupied molecular orbital (LUMO) gap between occupied ($\varepsilon_{i^{20}}$) and unoccupied ($\varepsilon_{g^{18}}$) orbitals for the Ag nanoparticle is $\Delta^{HOMO-LUMO} = \varepsilon_{1i^{20}} - \varepsilon_{2g^{18}} = 1.58$ eV.

It is well known that Ag aggregates are formed in a colloidal aqueous solution of NaCl (Ref. 7). Therefore studying electronic properties of small metallic particles in different dielectric matrices[32–34] presents a great scientific and practical interest as well as those of free Ag nanoparticles. When a metallic particle is placed in a dielectric medium, polarization changes $\rho_{pol}(\mathbf{r})$ are induced on the particle surface, which produce the potential

$$V_{pol}(\mathbf{r}) = 2 \int \frac{\rho_{pol}(\mathbf{r}')}{|\mathbf{r} - \mathbf{r}'|} d\mathbf{r}'. \quad (15)$$

In Ref. 33, we have shown that the ground state of a metal nanoparticle embedded in a dielectric matrix can be described by the self-consistent Kohn-Sham equations with the effective potential

$$V^{\varepsilon}(\mathbf{r}) = V(\mathbf{r}) + V_{pol}(\mathbf{r}), \quad (16)$$

where $V(\mathbf{r})$ has the same form as the effective potential for the nanoparticle in a vacuum. Averaging $V_{pol}(\mathbf{r})$ and substituting the result into Eq. (16) yields

$$V^{\varepsilon}(r) = \begin{cases} V(r) + \frac{1-\epsilon}{\epsilon} V(r_M) & r \leqslant r_M, \\ V(r)/\epsilon & r \geqslant r_M. \end{cases}$$

The calculations for the Ag_{125} nanoparticle embedded in a dielectric medium with the relative permeability $\epsilon = 61.1$ (50% water solution of NaCl) have shown that with the increasing dielectric permeability ϵ the potential profile near the jellium edge becomes steeper. The bottom of the potential well V_{bottom} and the single electron energy levels ε_i rise when the cluster is embedded in a dielectric matrix. It should be emphasized that the oscillations[33] in the electronic density of jellium cluster in vacuum are suppressed in the dielectric media. The amount of the electronic charge beyond the jellium edge (electronic "spill out") increases with the increasing ϵ. This is caused by a positive shift of the electronic eigenenergies of Ag nanoparticles in a dielectric medium and an extension of the corresponding wave functions.

The static dipole polarizability[35] is also well known to be intimately related to the electronic structure of a nanocluster.[33] We discuss here the photoresponse of an isolated Ag nanoparticle to an external electromagnetic field in terms of the frequency-dependent polarizability[36]

$$\alpha(\omega) = -\frac{8\pi}{3} \int_0^{\infty} dr' r'^3 \delta\rho(r', \omega), \quad (17)$$

where $\delta\rho(r', \omega)$ is the change in the charge density. The calculation of the static dipole polarizability $\alpha(\omega = 0)$ for an Ag nanoparticle is carried out within the time-dependent local-density approximation (TDLDA)[35] using the self-consistent solution of the set of equations

$$\delta\rho(\mathbf{r}, \omega) = \int \chi_0(\mathbf{r}, \mathbf{r}'; \omega) \delta V(\mathbf{r}') d\mathbf{r}', \quad (18)$$

$$\delta V(\mathbf{r}, \omega) = V_{ext}(\mathbf{r}, \omega) + V_{ind}(\mathbf{r}, \omega), \quad (19)$$

and

$$V_{ind}(\mathbf{r}, \omega) = 2 \int \frac{\delta\rho(\mathbf{r}', \omega)}{|\mathbf{r} - \mathbf{r}'|} d\mathbf{r}' + \frac{\partial V_{xc}(\mathbf{r})}{\partial\rho(\mathbf{r})} \delta\rho(\mathbf{r}, \omega). \quad (20)$$

Here $V_{ext}(\mathbf{r}, \omega)$ and $V_{ind}(\mathbf{r}, \omega)$ are the external field with the frequency ω and the induced field, respectively; $\chi_0(\mathbf{r}, \mathbf{r}'; \omega)$ is the susceptibility function in the independent-particle approximation. For $r_M = 15.1178$ a.u. (Ag_{125} cluster) $\alpha(\omega = 0) = 4.82 Å^3$/atom. The bulk atomic polarizability is 4.33 $Å^3$/atom.[37]

IV. RESULTS AND DISCUSSION

We present here a theoretical approach to the organic molecules interacting with silver in terms of numerically solvable DFT models. In practice, these models apply to nanosystems (PIC molecule on an Ag particle) and provide an understanding of doping silver nanoparticles by PIC adsorbates. The chemical structure of PIC molecule is exhibited in Fig. 2. The density-functional calculations are performed to determine the equilibrium structure of these PIC molecules by the DFT/B3LYP/6-31G-method.[17] The molecule geometries are optimized using the B3LYP-exchange-correlation energy functional and potential. The minimum basis set is capable of producing reasonable results is 6-31G. Since the geometry of PIC within the Ag + PIC nanosystem is undoubtedly disturbed as compared to the PIC monomer and possibly resembles a PIC aggregate, these calculations were performed as follows. First, the equilibrium geometry of the tetramer $(PIC : Cl)_4$ was found. After that, the averaged geometry of the monomer (PIC : Cl) was obtained by averaging over four molecules of the tetramer. The search of the equilibrium geometry of tetramer was performed by standard density functional method

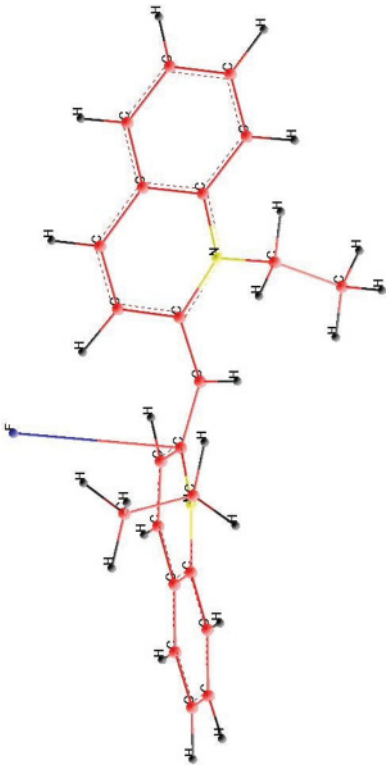

FIG. 2. (Color online) Configuration of the PIC molecule calculated by DFT/B3LYP/6-31G method: H (black) stand for the hydrogen atoms; C (red) stands for the carbon atoms; N (yellow) stands for the nitrogen atoms; F (blue) stands for the fluorine atom.

DFT/B3LYP/6-31G using the GAMESS program package.[17] The electronic structure of a neutral PIC molecule was calculated by the ZINDO/S method.[16]

It is assumed that the PIC molecule is adsorbed on the spherical surface of an Ag nanoparticle, setting down over the sphere so that its central carbon atom (the molecule center of gravity) is positioned in the point (2.223,0.680,0.705) Å, with respect to the center of the Ag nanoparticle. In the beginning we present the results of calculation of the electronic structure of an Ag_{125} nanoparticle obtained by the model of an *atom in the center of a spherical jellium sphere* and DFT in the LDA. Figure 1 presents the energy level structure of the Ag jellium nanoparticle with 134 valence electrons (the Ag atom core electrons orbitals lie below $\varepsilon_{3p^{3/2}} = -4.27$ Ry).

Figure 3 shows the Ag bound states by the red line. The peak heights are proportional to the degeneracy. The continuum density of states $\Delta n(\varepsilon)$ is given for the positive energies corresponding to the delocalized (unoccupied) states by Eq. (A18). Figure 3 exhibits the contribution of potential scattering [Eq. (A17)] to the formation of Ag related bound states ($\varepsilon_{2g} = -1.34$ eV) and fall in the broad range $\Delta^{\text{HOMO-LUMO}}$. This level is obtained from Eq. (A17) with $\widetilde{\mathcal{M}}$ substituted for Q^{-1} [see Eq. (A11)]. The states $2d^{10}(4d^{3/2} + 4d^{5/2})1f^{14}1g^{18}1h^{22}2f^{14}1i^{26}1j^{30}$ in the occupied part of the spectrum are the Ag resonances in the band (red line in Fig. 3) and lie in the interval $(-10, -5)$ eV. The resonant ε_{2g} level [see Fig. 3] arises at the energy 0.24 eV below the LUMO level. Both the Ag resonances and ε_{2g} states are found in the solution of Eq. (A17) with the full self-energy $\widetilde{\mathcal{M}}(z)$.

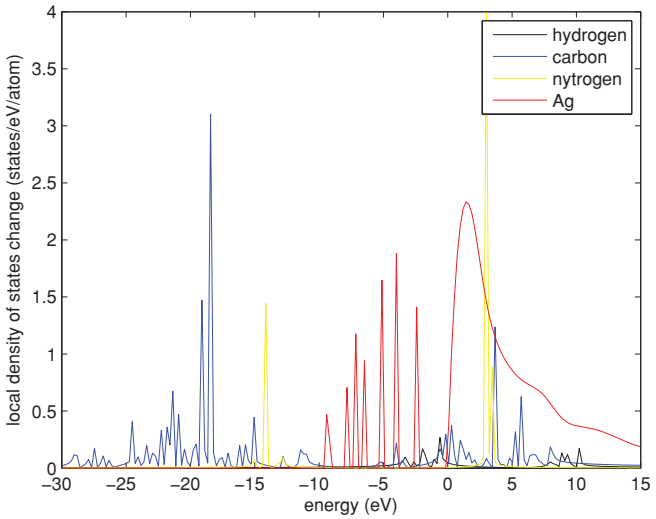

FIG. 3. (Color online) Density of states and Kohn-Sham level structure for nanosystem Ag + PIC.

The calculation of Ag_{125} particle embedded in a dielectric medium with relative dielectric permeability $\varepsilon = 61.1$ (50% water solution of NaCl) has shown that the electronic "spill out" increases in the dielectric medium as compared to vacuum and is equal for this case to 21.6 electrons.

The 26.14 eV width band of the Ag + PIC nanostructure is formed by strongly hybridized C(s, p) (blue line), N(s, p) (yellow line), H(s) (black line), and Ag (red line) states. The unoccupied states lie above $\varepsilon^{\text{LUMO}} = -1.58$ eV. Furthermore, we find the acceptor-like ε_{2g} states almost entirely localized in the adsorbate PIC molecule and hybridized with the hydrogen $1s$ levels. As discussed in Ref. 38, the interaction between the adsorbate and the transition metal surface can be described as a two-state problem (adsorbate state and the d band) leading to formation of bonding and antibonding states. Thus, an upshift of the d states should increase the adsorbate-metal interaction since it would lead to the formation of an antibonding orbital closer to the Fermi level. Strong features appearing between -5 and -10 eV represent the formation of a bonding orbital through the interaction of hydrogen $1s$ state with the metal d band, and this formation is typical for all transition metals. The bonding Ag $2d$-$1s$ states lie around -9 eV. The antibonding orbital lies around $\varepsilon^{\text{LUMO}}$ level and is hybridized with the resonance ε_{2g} states.

We will interpret the density of states (see Fig. 3) of the nanosystem Ag + PIC species based on their bonding properties obtained from the Green's function calculations and simple molecular orbital considerations. For a more detailed study of the chemical bonding in these nanosystems we have calculated the electron-density change $\Delta\rho(\mathbf{r})$ (see Fig. 4).

The electronic structure obtained for the Ag + PIC nanosystem has a terminal Ag–C bond. Similarly to all transition metals[39] the C–C bond is known to be much stronger than the Ag–C bond. Thus, it is not energetically favorable for Ag to enter the C chain since this will break the stronger C–C bonds and form weaker Ag–C bonds. The Green's function calculations indicate that the excited Ag atoms in the nanosystem are involved in the chemical bonding. Simple molecular orbital considerations suggest that

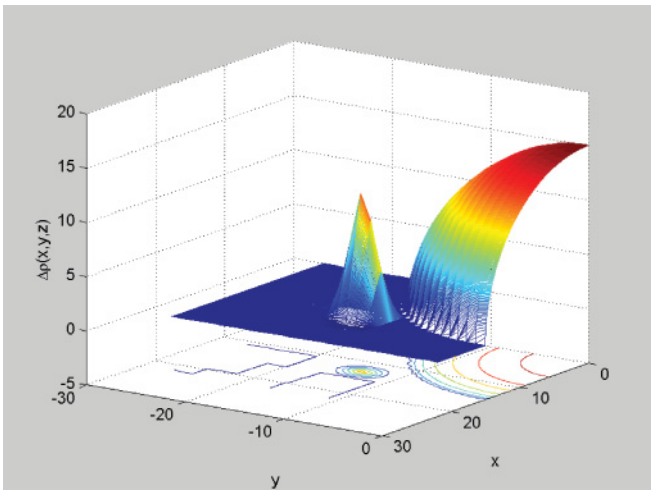

FIG. 4. (Color online) Difference electron-density charge for PIC molecule adsorbed on an Ag nanoparticle. The contours are in units of $10^{-5}e/\Omega_A$.

the C atom directly bonded to an Ag atom must be in an sp-hybridized state to more effectively interact with the Ag particle orbitals. And the Ag $2d$ orbitals can interact with the other p orbitals of the C atoms to form additional bonds. Thus, our calculations show that the Ag(d,s)–C(s,p) bond is of a considerable importance for understanding the nature of chemical bonding of the Ag + PIC nanosystem.

As shown in Fig. 3, all Ag states are situated between the C states. From the $\Delta n(\varepsilon)$ distribution as well as from its partial components $\Delta n_s(\varepsilon)$, $\Delta n_p(\varepsilon)$, and $\Delta n_d(\varepsilon)$, one can conclude, that the d-s,p resonance is observed in the (Ag + PIC) nanosystem, was revealed in the compounds of metals, containing the filled d shells, with nonmetals.[40] In this case,the Ag $5s$-type states $(1f^{14}1g^{18}1h^{22}2f^{14}1i^{26}1j^{30})$ form σ bonding and σ^* antibonding orbitals with the C sp hybridized orbitals. At the same time, the $2d\pi$ orbitals in Ag can interact with the C–C π orbitals. The resonance of the HOMO ε_{2g} with the hydrogen level (σ^* symmetry) is the principle interaction in the Ag$5s$–H$1s$ bond. This bond plays the crucial part in determining the chemisorption reactivity.[41]

There are two factors that affect this orbital interaction, first the HOMO energy and second, and more importantly, the symmetry of the HOMO. It follows from Ref. 41 that the d-symmetry HOMO would lead to a high reactivity. However, the ε_{2g} HOMO is mainly of $5s$ character and is not symmetry matched with the H σ^* orbital, hence it results in an extremely low reactivity. Thus, the s-type HOMO of the Ag + PIC nanosystem effectively provides a *shielding effect* to protect the nanosystem from being attacked by the hydrogen atoms.

Figure 4 shows the charge density difference of an Ag + PIC nanosystem

$$\Delta\rho(\mathbf{r}) = \rho^{\mathrm{Ag+PIC}}(\mathbf{r}) - \rho^{\mathrm{Ag}}(\mathbf{r}) - \sum_a \rho_a^{\mathrm{atom}}.$$

Here, $\rho^{\mathrm{Ag+PIC}}(\mathbf{r})$ is the self-consistent electron density of the Ag + PIC nanosystem; ρ_a^{atom} is the electron density of the free atoms in the PIC molecule; $\rho^{\mathrm{Ag}}(\mathbf{r})$ is the density in reference system. The Ag sphere with radius 15.12 a.u. is also schematically shown. The electron-density charge is close to $z = 1.33$ a.u. Figure 4 reveals that the electron density change $\Delta\rho(\mathbf{r})$ is strongly localized. We see also that the adsorbed PIC molecule causes an accumulation of the reference charge on the Ag metal side due to the three carbon atoms with the coordinates (14.21, −13.71,1.33) a.u., (12.13,−12.03,0.99) a.u., (13.93,−16.37,1.31) a.u. and one hydrogen atom with the coordinates (15.25,−17.37,2.26) a.u. Based on the chemical bonding model of the carbon and hydrogen valences, the chemical structure of interaction between the Ag and (C,H) atoms of the PIC molecule has the form

$$\text{H–Ag–C} = \text{C–C–H}.$$

The major part of the electron density in C=C and C=N bonds is localized at the bottom of the band and has the sp and sp^2 type covalence of the chemical bonding. At the same time, the upper part of the occupied states contain mainly the bonding electrons which are concentrated in Ag–H and Ag–C bonds and have (d,s)–(s,p) resonance type of bonding with the maximum displacement toward the Ag nanoparticle.

V. CONCLUDING REMARKS

Carrying out a numerical solution of the Dyson equation (A11) in the Kohn-Sham density-functional methodology we determined the electronic and chemical structure of Ag + PIC nanosystems. The calculation of the Ag_{125} particle embedded in a dielectric medium with the relative permeability $\epsilon = 61.1$ (50% water solution of NaCl) shows that the amount of the electronic charge beyond the jellium edge (electronic "spill out") increases in the dielectric medium as compared to the vacuum and equals in this case 21.6 electrons. The resonant ε_{2g} level (see Fig. 3) arises at the energy 0.24 eV under the LUMO level. Both the Ag resonances and ε_{2g} states are found as solutions of Eq. (A17) with the full self-energy $\widetilde{\mathcal{M}}(z)$. The electronic structure obtained for the Ag + PIC nanosystem has a terminal Ag–C bond.

Three C atoms and one H atom take part in the adsorption of the PIC molecule on the Ag nanoparticle and accumulation $\Delta\rho$ of charge takes place. The hybridized Ag–H and Ag–C bonds are of the (d,s)-(s,p) resonance type with the maximal displacement of charge toward the Ag nanoparticle.

ACKNOWLEDGMENTS

The authors are indebted to K. Kikoin for detailed discussions. This work was supported by the Russia-Israel Scientific Research Cooperation, Grant No. 3-5802 (B.F. and V.M.) and the Israel-US Binational Science Foundation (B.F.), Grant No. 2008282.

APPENDIX: GREEN'S FUNCTION TECHNIQUE TO CALCULATE THE ELECTRONIC PROPERTIES OF ORGANIC ADMOLECULE ON METAL CLUSTER

Our approach is based on the general concept formulated in Ref. 42. It makes it possible to calculate the electronic structure of metallic substrates and to study the behavior of a compact cluster adsorbed on a nanoparticle. The principal

theoretical tool is the scattering theory formalism, which considers perturbation of a metal substrate single electron potential by a spatially compact cluster, which is itself compact by virtue of screening. It can therefore be treated as a localized scattering potential for Ag electrons of the substrate. To obtain the electronic structure of the admolecule on an Ag nanoparticle a "matrix" scattering approach is adopted. Our objective is to construct the Green's function matrix $G_{\mu\nu}(z)$ for the perturbed system (e.g., silver nanoparticle with organic PIC molecule).

The theoretical analysis providing us with a link between the nanosystem and the related simple systems (Ag nanoparticle and PIC molecule) is based on the Dyson equation (7). As is well known, the original problem of solving a linear differential equation can be mapped onto the solution of a matrix equation of an infinite dimension by expanding the wave functions in terms of a linear combination of properly chosen orthonormal functions, for example, the atomic orbitals (LCAO's) that are used here. In most cases of the LCAO cluster calculations Slater-type orbitals strongly facilitate the numerical calculation of overlap integrals.

In practical calculations we construct the Green's function matrix $G_{\mu\nu}(z)$ (6) using a finite set of N_b basis functions $\chi_\mu(\mathbf{r})$. The basis set only needs to cover the real space, within which $\Delta\rho(\mathbf{r})$ is localized. We will denote this region as box A of volume Ω_A. In the present implementation of our method the $\chi_{nlm}(\mathbf{r})$ are the Kohn-Sham orbitals

$$\chi_{nlm}(\mathbf{r}) = \psi_{nl}(|\mathbf{r}-\mathbf{R}_\alpha|)Y_{lm}(\theta_{\mathbf{r}-\mathbf{R}_\alpha},\phi_{\mathbf{r}-\mathbf{R}_\alpha}), \tag{A1}$$

placed at appropriately chosen positions $\mathbf{R}_\alpha$ in the PIC assembled molecule. Here we choose the basis of atomic functions so that $\mu \equiv nml$. $\psi_{nlm}(\mathbf{r})$ are the Kohn-Sham radial wave functions obtained with the help of the potential $\Delta V(\mathbf{r})$, which, in turn, is calculated by means of the functions $\psi_{nlm}(\mathbf{r})$. The self-consistency iterations are repeated until a desired convergence is achieved. $Y_{lm}(\theta,\phi)$ are the spherical harmonics centered at $\mathbf{R}_\alpha$.

Writing the Dyson equation

$$\mathsf{G}(z) = \mathsf{G}^0(z) + \Delta\mathsf{G}(z), \tag{A2}$$

we see that only the difference operator $\Delta\mathsf{G}(z)$ [and the difference electron charge density $\Delta\rho(\mathbf{r})$ related to it] need to be be actually calculated. This difference operator has the form

$$\Delta\mathsf{G}(z) = [(\mathsf{I} - \widetilde{\mathsf{G}}^0(z)\cdot\Delta\mathcal{V}\cdot(\mathsf{L}^{-1})^\dagger)^{-1} - \mathsf{I}]\widetilde{\mathsf{G}}^0(z),$$

where

$$\Delta\mathcal{V}_{\mu\nu} = \int_{\Omega_A}\chi^*_\mu(\mathbf{r})\Delta V[\rho(\mathbf{r})]\chi_\nu(\mathbf{r})d\mathbf{r},$$

and I is a unit matrix. Here the factor L^{-1} ensues from the assumption that the basis set $\chi_\mu(\mathbf{r})$ was used in the Cholesky decomposition $\mathsf{S} = \mathsf{L}\cdot\mathsf{L}^\dagger$ for the overlap matrix

$$S_{\mu\nu} = \int_{\Omega_A}\chi^*_\mu(\mathbf{r})\chi_\nu(\mathbf{r})d\mathbf{r},$$

to obtain the orthonormal basis.

The density variation is calculated using the equation

$$\Delta\rho(\mathbf{r}) = \mathrm{Im}\sum_{\mu=1}^{N_b}\sum_{\nu=1}^{N_b}\widetilde{\Delta\rho}_{\mu\nu}\chi_\mu(\mathbf{r})\chi^*_\nu(\mathbf{r}), \tag{A3}$$

where

$$\widetilde{\mathsf{G}}^0_{\mu\nu}(z) = ((\mathsf{L}^{-1})^\dagger\mathsf{G}^0(z)\mathsf{L}^{-1})_{\mu\nu},$$
$$\widetilde{\Delta\rho}_{\mu\nu} = ((\mathsf{L}^{-1})^\dagger\Delta\rho\mathsf{L}^{-1})_{\mu\nu},$$

and

$$\Delta\rho = -\frac{1}{\pi}\int_{\varepsilon_b}^{\varepsilon_{\mathrm{HOMO}}}\Delta\mathsf{G}(z)dz. \tag{A4}$$

The lower integration limit ε_b is chosen in such a way as to include all the relevant Ag and molecule states, $\varepsilon_{\mathrm{HOMO}}$ is the HOMO energy. To compute the integral (A4), we introduce a contour C in the complex plane z enclosing all the poles of the Green's function up to the HOMO's energy in the charge density integration.

Our computational scheme is based on the spherically symmetric Ag metallic nanoparticle Green's function

$$G^0(\mathbf{r},\mathbf{r}';\varepsilon) = \sum_{lm}Y_{lm}(\theta,\phi)G^0_l(r,r';\varepsilon)Y^*_{lm}(\theta',\phi'), \tag{A5}$$

decomposed in terms of the spherical harmonics.[35] Here

$$G^0_l(r,r';\varepsilon) = \frac{R_l(r_<,\varepsilon)N_l(r_>,\varepsilon)}{r^2W_l(\varepsilon)}, \tag{A6}$$

with $r_< = \min(r,r')$,$r_> = \max(r,r')$. $R_l(r_<,\varepsilon)$ and $N_l(r_>,\varepsilon)$ are the regular and nonregular solutions of the radial Kohn-Sham equations with the potential $V^0(r)$ and energy ε. $W_l(\varepsilon)$ is the Wronskian of the functions R_l and N_l. We obtain R_l and N_l by integrating the radial Kohn-Sham equation, using the asymptotic behavior of these functions at the origin and infinity. As is generally known, the regular solution R_l behaves asymptotically as r^{l+1} at $r \to 0$. When $r \to \infty$, the nonregular solution N_l must be an outgoing wave for the continuum-energy region($\varepsilon > 0$), and it exponentially decreases for the bound-state region ($\varepsilon < 0$).

The Green's function of the nanoparticle is projected onto the localized basis

$$G^0_{\mu\nu}(\varepsilon) = \sum_{lm}\langle\mu|\Theta_A|R_l(r_<,\varepsilon)\rangle\langle N_l(r_>,\varepsilon)|\Theta_A|\nu\rangle/W_l(\varepsilon). \tag{A7}$$

The following notations have been used above

$$\langle\mu|\Theta_A|R_l(r_<,\varepsilon)\rangle = \int_{\Omega_A}\chi^*_\mu(\mathbf{r}-\mathbf{R}_\alpha)R_l(r_<,\varepsilon)d\mathbf{r},$$
$$\langle N_l(r_>,\varepsilon)|\Theta_A|\nu\rangle = \langle\nu|\Theta_A|N_l(r_>,\varepsilon)\rangle^*,$$
$$\langle\nu|\Theta_A|N_l(r_>,\varepsilon)\rangle = \int_{\Omega_A}\chi^*_\nu(\mathbf{r}-\mathbf{R}_\beta)N_l(r_>,\varepsilon)d\mathbf{r},$$
$$\Theta_A(\mathbf{r}) = \begin{cases}1, & \mathbf{r}\in\Omega_A - \text{volume of the box region A}\\ 0, & \text{otherwise}\end{cases}$$

Here we use the single-center method to compute all integrals in the Slater-type orbital basis.[43] The Slater orbital centered in a point, defined by its location vector $\mathbf{R}_\alpha$, is usually

$$\chi_{nlm}(\mathbf{r}) = N_{nl}|\mathbf{r}-\mathbf{R}_\alpha|^{n-l-1}\exp(-\zeta|\mathbf{r}-\mathbf{R}_\alpha|) \times Y_{lm}(\theta_{\mathbf{r}-\mathbf{R}_\alpha},\phi_{\mathbf{r}-\mathbf{R}_\alpha}). \quad \text{(A8)}$$

The radial part of the Slater orbital is expanded over the Barnett-Coulson/Löwdin function (BCLF)[44]

$$|\mathbf{r}-\mathbf{R}_\alpha|^{n-l-1}\exp(-\zeta|\mathbf{r}-\mathbf{R}_\alpha|) = \frac{1}{\sqrt{R_\alpha r}}\sum_\lambda (2\lambda+1)\mathcal{A}^{n-l}_{\lambda+1/2}(\zeta,R_\alpha,r)P_\lambda\left(\frac{\mathbf{R}_\alpha\cdot\mathbf{r}}{R_\alpha r}\right), \quad \text{(A9)}$$

where $P_n(z)$ are the Legendre polynomials of degree n and $\mathcal{A}^{n-l}_{\lambda+1/2}(\zeta,R_\alpha,r)$ are the BCLF's defined by the recursion

$$\mathcal{A}^n_{\lambda+1/2}(\zeta,R_\alpha,r) = -\frac{\partial}{\partial\zeta}\mathcal{A}^{n-l}_{\lambda+1/2}(\zeta,R_\alpha,r),$$

with

$$\mathcal{A}^0_{\lambda+1/2}(\zeta,R_\alpha,r) = \mathbf{I}_{\lambda+1/2}(\zeta\rho_<)\mathbf{K}_{\lambda+1/2}(\zeta\rho_>),$$

where $\mathbf{I}_{\lambda+1/2}(z)$ and $\mathbf{K}_{\lambda+1/2}(z)$ are the modified Bessel functions of the first and second kinds; the variables $\rho_<$ and $\rho_>$ stand for the $\min(R_\alpha,r)$ and $\max(R_\alpha,r)$, respectively. In the present implementation of our method the Kohn-Sham orbitals are placed at appropriately chosen positions $\mathbf{R}_\alpha$.

Information on the Ag + PIC adsorption can be produced from the Dyson Eq. (7) that describes the interaction between the free molecule and silver particle. In this Dyson equation the part of the unperturbed Green's function is played by the *augmented Green function*

$$\mathsf{G}^{NS}_{\mathrm{Ag+PIC}}(z) = \begin{pmatrix} G^0_{\mathrm{PIC}}(z) & 0 \\ 0 & G^0_{\mathrm{Ag}}(z) \end{pmatrix}. \quad \text{(A10)}$$

To describe the molecule–silver nanoparticle interaction we use the approach known in the theory of transition metal impurities in semiconductors.[12,45–48] The terms in the model Hamiltonian (2) for the Ag + PIC nanosystem are written as

$$H^r_{\mathrm{PIC-Ag}} = \sum_{ki_a} M_{ki_a}c^\dagger_k d_{i_a} + \mathrm{h.c.},$$

and

$$H^p_{\mathrm{PIC-Ag}} = \sum_{kk'} W_{kk'}c^\dagger_k c_{k'}.$$

Here, c_k (d_{i_a}) and $c^\dagger_k$ ($d^\dagger_{i_a}$) denote the usual fermionic annihilation and creation operators, respectively, which are labeled by the indexes k and i_a containing site, orbital, and spin degrees of freedom; M_{ki_a} is the $s,d-i_a$-hybridization matrix element, and $W_{kk'}$ is the matrix element for the Ag particle short-range potential scattering (the subscript "a" refers to the ath adatom in the PIC admolecule and i_a stands for the corresponding electronic state and atom site). The Dyson equation reads

$$G_{i_ai_a}(z) = G^{NS}_{i_ai_a}(z)\left[1+\widetilde{\mathcal{M}}_{i_a}(z)G_{i_ai_a}(z)\right], \quad \text{(A11)}$$

where

$$G^{NS}_{i_ai_a}(z) = \frac{1}{z-\varepsilon_{i_a}-\Delta V_{i_ai_a}},$$
$$\widetilde{\mathcal{M}}_{i_a}(z) = \mathcal{M}_{i_a}(z)Q^{-1}(z).$$

Off-diagonal elements even for the nearest neighbors are up to two orders of magnitude smaller than the diagonal ones and are neglected.

The PIC electron levels ε_{i_a} are found self-consistently as solutions of the Kohn-Sham equations for the PIC related orbitals in the nanosystem environment. The self-energy $\mathcal{M}_{i_a}(z)$ contains two contributions. The term

$$\mathcal{M}_{i_a}(z) = \sum_k \frac{|M_{ki_a}|^2}{z-\varepsilon_k}, \quad \text{(A12)}$$

describes the hybridization between the s,d PIC orbitals (ψ_{i_a}) and the Ag electrons (ψ_k) with the matrix element

$$M_{ki_a} = \int_{\Omega_A}\psi^*_k(\mathbf{r})\Delta V(\mathbf{r})\psi_{i_a}(\mathbf{r}-\mathbf{R}_\alpha)d\mathbf{r}. \quad \text{(A13)}$$

The factor

$$Q(z) = 1-\Delta V_{\mathrm{pot}}G^0_{\mathrm{Ag}}(z), \quad \text{(A14)}$$

in Eq. (A11) describes the short-range potential scattering, where

$$\Delta V_{\mathrm{pot}} = \sum_{kk'}\int\psi^*_k(\mathbf{r})\Delta V(\mathbf{r})\psi_{k'}(\mathbf{r})d\mathbf{r}, \quad \text{(A15)}$$

and

$$G^0_{Ag}(z) = \sum_k\langle k|\left(z-H^0_{\mathrm{LDA}}\right)^{-1}|k\rangle = \sum_k\frac{1}{z-\varepsilon_k}, \quad \text{(A16)}$$

is the single-site lattice Green's function for the electrons in the Ag host cluster described by the Hamiltonian H^0_{LDA}.

The Ag electron levels ε_k are found self-consistently as solutions of the Kohn-Sham equations for the Ag-related orbitals in the nanosystem environment. The Green's function (A11) describes the hybridization between the PIC electron orbitals and the electrons in the silver host cluster, where the Ag electrons are influenced by the potential scattering due to ΔV. If this scattering is strong enough, it results in the splitting off of localized levels from the top of the band. This effect is also taken into account in Eq. (A11): the positions of the corresponding levels before the hybridization are determined by the zeros of the function $Q(z)$ in the energy gap $\Delta^{\mathrm{HOMO\text{-}LUMO}}$ of the Ag + PIC nanosystem, which arises in the electronic structure due to the potential scattering only. As a result the equation for the deep level energy determined as a pole of the Green's function [Eq. (A11)] within the framework of the LDA technique reads

$$z-\varepsilon_{i_a}-\Delta V^{\mathrm{LDA}}_{i_ai_a} = \widetilde{\mathcal{M}}_{i_a}(z). \quad \text{(A17)}$$

It takes into account the resonance part of the scattering amplitude in the i_a (PIC) channel and its mixing with the potential scattering states arising in the k (Ag) channel.

The imaginary part of the Green's function yields the spatial and energy electron distribution

$$\rho(\mathbf{r},\varepsilon) = -\frac{2}{\pi}\mathrm{Im}G(\mathbf{r},\mathbf{r};\varepsilon).$$

Integrating over the energy we get the charge density distribution, whereas the local density of states (e.g., in the cell Ω_A) reads

$$n_{\mathrm{loc}}(\varepsilon) = \int_{\Omega_A} \rho(\mathbf{r},\varepsilon)d\mathbf{r}.$$

The change of the density of states is

$$\Delta n(\varepsilon) = \mathrm{Tr}(G_{\mathrm{Ag+PIC}}) - \mathrm{Tr}(G^0_{\mathrm{Ag}}),$$

or after straightforward calculations

$$\Delta n(\varepsilon) = \frac{2}{\pi}\mathrm{Im}\sum_{i_a}\frac{d}{d\varepsilon}\ln\left[\left(z-\varepsilon_{i_a}-\Delta V_{i_a i_a}\right)Q(\varepsilon)-\mathcal{M}_{i_a}(z)\right]. \tag{A18}$$

The problem is treated self-consistently, starting with the trial set of LCAO Slater-type functions. The difference potential in the zero approximation is a sum of the atomic potentials of the nanosystem. The self-consistency procedure for $\Delta V(\mathbf{r})$ is carried out in a mixed fashion. The first two iterations use the arithmetic average scheme, which later on is effectively substituted by the Aitken scheme.[26] Just seven iterations produce a 10^{-4} Ry self-consistency.

[1] G. P. Wiederrecht, G. A. Wurtz, and J. Hranisavljevic, Nano Lett. **4**, 2121 (2004).
[2] F. Evers, F. Weigend, and M. Koentopp, Phys. Rev. B **69**, 235411 (2004).
[3] C. M. Aikens and G. C. Schatz, J. Phys. Chem. A **110**, 13317 (2006).
[4] A. Nitzan and M. A. Ratner, Science **300**, 1384 (2003).
[5] K. Kneipp, H. Kneipp, and M. Rentsch, J. Mol. Struct. **156**, 331 (1987).
[6] I. Renge and U. P. Wild, J. Phys. Chem. A **101**, 7977 (1997).
[7] Y. Tanaka, H. Yoshikawa, T. Itoh, and M. Ishikawa, J. Phys. Chem. C **113**, 11856 (2009).
[8] L.-J. Wan, Acc. Chem. Res. **39**, 334 (2006).
[9] W. Kohn and L. J. Sham, Phys. Rev. **140**, A1133 (1965)
[10] O. V. Farberovich, A. Yaresko, K. Kikoin, and V. Fleurov, Phys. Rev. B **78**, 085206 (2008).
[11] P. Hohenberg and W. Kohn, Phys. Rev. **136**, B864 (1964).
[12] K. A. Kikoin and V. N. Fleurov, *Transition Metal Impurities in Semiconductors* (World Scientific, Singapore, 1994).
[13] L. I. Kurkina and O. V. Farberovich, J. Phys.: Condens. Matter. **4**, 6417 (1992).
[14] M. Scheffler, Ch. Droste, A. Fleszar, F. Maca, G. Wachutka, and G. Barzel, Physica B **172**, 143 (1991).
[15] G. Wachutka, A. Fleszar, F. Maca, and M. Scheffler, J. Phys.: Condens. Matter. **4**, 2831 (1992).
[16] M. C. Zerner, G. H. Loew, R. F. Kirchner, and U. T. Mueller-Westenhoff, J. Amer. Chem. Soc. **102**, 589 (1980).
[17] M. W. Schmidt, K. K. Baldridge, J. A. Boatz, S. T. Elbert, M. S. Gordon, J. J. Jensen, S. Koseki, N. Matsunaga, K. A. Nguyen, S. Su, T. L. Windus, M. Dupius, and J. A. Montgomery, J. Comput. Chem. **14**, 1347 (1993).
[18] F. Baletto, C. Mottet, and R. Ferrando, Phys. Rev. B **63**, 155408 (2001).
[19] H. Haberland, *Clusters of Atoms and Molecules, (Theory, Experiments, and Clusters of Atoms)* (Springer, Berlin, 1994).
[20] M. Acherman, J. Phys. Chem. Lett. **1**, 2837 (2010).
[21] W. Ekardt, Phys. Rev. B **29**, 1558 (1984).
[22] L. I. Kurkina, O. V. Farberovich, and V. A. Gorbunov, J. Phys.: Condens. Matter. **5**, 6029 (1993).
[23] S. H. Vosko, L. Wilk, and M. Nussiar, Can. J. Phys. **58**, 1200 (1980).
[24] W. E. Milne, Amer. Math. Monthly **33**, 455 (1926).
[25] O. V. Farberovich, S. V. Vlasov, and G. P. Nizhnikova, Program of the self-consistent relativistic calculation of the atomic and ionic structures in LSDA approximation, VINITI No. 2953–83, (1983) (Russia).
[26] A. C. Aitken, Proc. R. Soc. Edinburgh Biol. **46**, 389 (1926).
[27] J. Conceicao, R. T. Laaksonen, L.-S. Wang, T. Guo, P. Nordlander, and R. E. Smalley, Phys. Rev. **51**, 4668 (1995).
[28] J. Slater, Adv. Quantum Chem. **6**, 1 (1972).
[29] J. F. Janak, Phys. Rev. B **18**, 7165 (1978).
[30] O. B. Christensen, K. W. Jacobsen, J. K. Norskov, and M. Manninen, Phys. Rev. Lett. **66**, 2219 (1991).
[31] M.-L. Bogouet, A. M. Rappe, and H.-L. Dai, Mol. Phys. **103**, 883 (2005).
[32] L. I. Kurkina and O. V. Farberovich, Z. Phys. D **37**, 359 (1996).
[33] L. I. Kurkina and O. V. Farberovich, Phys. Rev. B **54**, 14791 (1996).
[34] J. Lerme, Eur. Phys. J. D **10**, 265 (2000).
[35] A. Zangwill and P. Soven, Phys. Rev. A **21**, 1561 (1980).
[36] M. J. Puska, R. M. Nieminen, and M. Manninen, Phys. Rev. B **31**, 3486 (1985).
[37] M. Pereiro and D. Baldomir, Phys. Rev. A **75**, 033202 (2007).
[38] B. Hammer and J. K. Norskov, Nature (London) **376**, 238 (1995)
[39] M. L. McKee, J. Am. Chem. Soc. **112**, 2601 (1990).
[40] O. V. Farberovich, Yu. K. Timoshenko, A. M. Bugakov, and E. P. Domashevskaya, Sol. St. Commun. **40**, 559 (1981).
[41] L.-S. Wang, H.-S. Chen, and J. Fan, Chem. Phys. Lett. **236**, 57 (1995).
[42] A. R. Williams, P. J. Feibelman, and N. D. Lang, Phys. Rev. B **26**, 5433 (1982).
[43] A. Bouferguene and D. Rinaldi, Int. J. Quantum Chem. **50**, 21 (1994).
[44] A. Bouferguene, J. Phys. A: Math. Gen. **38**, 2899 (2005).
[45] V. N. Fleurov and K. A. Kikoin, J. Phys. C **19**, 887 (1986).
[46] P. W. Anderson, Phys. Rev. **124**, 41 (1961).
[47] V. N. Fleurov and K. A. Kikoin, J. Phys. C: Solid State Phys. **9**, 1673 (1976).
[48] F. D. M. Haldane and P. W. Anderson, Phys. Rev. B **13**, 2553 (1976).